Journal of Veterinary Internal Medicine
Open Access
J Vet Intern Med 2016;30:714–721

Speckle-Tracking Echocardiography in Dogs With Patent Ductus Arteriosus: Effect of Percutaneous Closure on Cardiac Mechanics

I. Spalla, C. Locatelli, A.M. Zanaboni, P. Brambilla, and C. Bussadori

Background: Patent ductus arteriosus (PDA) is 1 of the most common congenital heart defects in dogs and percutaneous closure is effective in achieving ductal closure; PDA closure is associated with abrupt hemodynamic changes.

Hypothesis: A marked decrease in standard parameters of systolic function as assessed by M- or B-mode echocardiography after PDA closure was identified in previous studies. Speckle tracking echocardiography can provide further insight into the effect of PDA closure on cardiac mechanics in dogs affected by PDA.

Animals: Twenty-five client-owned dogs with PDA.

Methods: Prospective study. Dogs were recruited over a 2-year period. Complete echocardiographic evaluation was performed before and 24 hours after PDA closure, including standard (end-diastolic volumes indexed to body surface area in B- and M-mode [$EDVI_{B/M}$], end-systolic volumes indexed to body surface area in B- and M-mode [$ESVI_{B/M}$], allometric scaling in diastole [AlloD] and systole [AlloS], pulmonary flow to systemic flow [Qs/Qp], ejection fraction [EF], and fractional shortening [FS]), and advanced speckle-tracking echocardiography (STE): global longitudinal, radial, circumferential and transverse strain (S), and strain rate (SR).

Results: Patent ductus arteriosus closure was associated with statistically significant decreases in $EDVI_{M/B}$ and $ESVI_{M/B}$, AlloD and AlloS, SI, EF, and FS. A statistically significant decrease in the absolute values of radial, transverse, and circumferential S and SR was observed, whereas longitudinal S and SR did not change significantly.

Conclusion and Clinical Importance: Patent ductus arteriosus closure by percutaneous approach is associated with marked decreases of conventional echocardiographic parameters as a result of the changes in loading conditions, but no evidence of systolic dysfunction was identified by means of STE, as none of the S and SR values were below reference ranges. In the short term, contractility is enhanced in the long axis (long S/SR values were not statistically different before and after closure) and decreases to normal values in short axis (circumferential, radial, and transversal S/SR decreased to normal reference range).

Key words: Congenital heart disease; Dogs; Strain; Strain rate.

The ductus arteriosus is a fetal vascular structure connecting the aorta to the main pulmonary artery and normally closes shortly after birth by a complex neurohormonal and hemodynamic process.[1] In dogs, patent ductus arteriosus (PDA) is an isolated heart defect that accounts for 21–32% of total congenital heart disease.[2–5] A left-to-right PDA is associated with pulmonary over circulation and left ventricular (LV) volume overload with increased preload soon after birth.[6–8]

Transcatheter interventional techniques are effective to close the PDA, and the Amplatz Canine Duct Occluder[a] (ACDO) is the device most commonly used in veterinary medicine because of its efficacy and low complication rate.[9,10] Data regarding the hemodynamic changes asssociated with percutaneous closure of PDA have been investigated by transthoracic echocardiography.[11–15] Dogs with PDA show increases in end-diastolic and end-systolic dimensions, which tend to decrease after PDA closure. Marked decrease in fractional shortening (FS) and ejection fraction (EF) are associated findings,[11–15] with some patients showing EF and FS values below reference ranges;[11–15] but no change in long-term survival was identified by previous studies.[14,15] The speculation that PDA closure in young patients may be accompanied by LV systolic dysfunction because of the inability of the LV to compensate for acute loading changes can be further investigated by advanced imaging modalities. Advanced echocardiographic techniques quantify cardiac contractility and deformation by direct assessment of cardiac motion.[16–22]

Abbreviations:

PDA	patent ductus arteriosus
STE	speckle-tracking echocardiography
$EDVI_M$	end-diastolic volume index derived from M-mode
$EDVI_B$	end diastolic volume index derived from B-mode
$ESVI_M$	end systolic volume index derived from M-mode
$ESVI_B$	end systolic volume index derived from B-mode
AlloD	allometric scale in diastole
AlloS	allometric scale in systole
FS	fractional shortening
EF	ejection fraction
Qs/QpQs/Qp	systemic flow to pulmonary flow ratio
S	strain
SR	strain rate

From the Università degli Studi di Milano, Milano, Italy (Spalla, Locatelli, Zanaboni, Brambilla); Clinica Veterinaria Gran Sasso, Milano, Italy (Bussadori).

Dogs with patent ductus arteriosus were scanned at Clinica Veterinaria Gran Sasso. Post-processing was performed by the corresponding author at Università degli Studi di Milano.

Corresponding author: I. Spalla, via padre lega 53, Gallarate, Italy; e-mail: illispa@hotmail.com.

Submitted July 2, 2015; Revised January 23, 2016; Accepted February 9, 2016.

DOI: 10.1111/jvim.13919

They have been promoted as complementary and more sensitive tools to evaluate cardiac function in a wide variety of clinical diseases in human cardiology.[20]

Speckle tracking echocardiography (STE) is 1 of the most common advanced imaging modalities in human cardiology, and it is based on a software algorithm that tracks speckles (natural acoustic markers in the myocardium) during the cardiac cycle based on 2-dimensional (2D) images.

The aim of our study therefore was to assess standard and advanced echocardiographic parameters in a population of young dogs affected by PDA both before and 24 hours after percutaneous closure to investigate the short term effect of percutaneous closure on cardiac mechanics.

Materials and Methods

Dogs were prospectively recruited at the Clinica Veterinaria Gran Sasso for ductal closure of isolated left-to-right PDA. Inclusion criteria included a complete medical record (signalment, physical examination, complete pre- and postoperative echocardiography, electrocardiogram, and radiography). Exclusion criteria were any additional congenital or acquired cardiac diseases and/or incomplete medical record .

All dogs underwent percutaneous closure by ACDO device. Postoperative echocardiography was performed 24 h after ductal closure.

A complete standard echocardiographic examination was performed in all dogs in accordance with published guidelines for human and veterinary medicine.[23,24] All echocardiographic examinations were performed using a commercial ultrasound equipment with 2.5–10 Mhz phase array ultrasound probes.

Standard echocardiographic parameters included: end-diastolic volume and end-systolic volume indexed to body surface area (EDVI and ESVI), measured by Teichholz method on M-mode ($EDVI_M$/$ESVI_M$), and area-length method on B-mode ($EDVI_B$/$ESVI_B$) and allometric scaling of LV M mode dimensions (AlloD and AlloS).[25] Furthermore, fractional shortening (FS) and ejection fraction (EF_M) in M-mode were determined. The EF also was calculated by B-mode using the area-length method from the apical 4-chamber view (EF_B). To provide additional information about shunt severity, Qs/Qp was measured as described.[26] Sphericity index (SI) was measured as described.[27]

At least 3 clips with 1 cardiac cycle additionally were acquired for STE postprocessing. Positive QRS eletrocardiographic (ECG) gating, good image quality and high frame rate (least acceptable frame rate: fps 80[28]) were deemed fundamental and thus frame rate, sector width and probe frequency were adjusted to optimize image acquisition.[28] To standardize short axis acquisitions, the basal plane was identified as containing mitral leaflets (right parasternal view at the level of mitral valve [MV]), while the mid-level was identified as containing the papillary muscles (right parasternal view at the level of the papillary muscles [PM]). Particular attention was given to make the LV cross-section as circular as possible and that transversal overlapping ("out-of-plane motion") was limited as much as possible. Long axis view (4Ch) was acquired by apical 4-chamber view, which should optimize LV length, endocardial borders, and should never include the LV outflow tract.[28]

Commercial[b] software was used for off-line analysis. The cineloop was evaluated by slow motion and a still frame was selected as a starting point (Fig 1A). Generally, end-diastole was the preferred timing for best visualization of endocardial borders and, where necessary, epicardial borders. The starting points for endocardial tracing were placed manually (2 at midplane both in MV and PM and 3 at the apical 4Ch view at both MV hinge points and cardiac apex [Fig 1B]), and then the software provided tracking guidance by the presence of drawn lines originating from the LV cavity where the endocardial border was manually identified and selected (for a total of 12 points in short axis views and 13 in long axis views [Fig 1C]). After selecting these points, the software automatically divided the myocardium into 6 segments, as shown by a continuously traced line (Fig 1D–E), which should follow the endocardial border and was manually adjusted to fit. Velocity vector imaging (VVI) arrows were then displayed above the endocardial border and helped evaluate tracking quality during the cardiac cycle (Fig 1F). When necessary, only 1 manual attempt to adjust endocardial points was considered acceptable. If VVI arrows showed unacceptable tracking quality, the cineloop was discarded. The procedure for epicardial tracking was the same as that for endocardial tracking.

After this procedure, strain (S) and strain rate (SR) curves were obtained by the software (Fig 2). No adjustment to the original tracking was done after obtaining the curves. Data then were exported to an Excel[c] data sheet and prepared for statistical analysis.

All echocardiographic values were measured 3 times on 3 different days by the same operator based on a single clip/image and the results shown are averaged.[28] For advanced echocardiographic values, a global S and SR are provided, which are the averaged value of the 6 regional segments identified by the software. Final S and SR values were obtained by an average of 3 consecutive measurements taken on 3 different days.[28] Circumferential S and SR were measured at the MV level, radial S and SR were measured by short axis view at the level of the PM, whereas transverse S and SR were obtained by the long axis view at the apical 4-chambers view Longitudinal S and SR were measured at the apical 4-chamber view. Epicardial S and SR were measured for longitudinal and circumferential displacement. A between-day and within-day coefficient of variation (CV) was randomly assessed in 30% of the patients.

Statistical Analysis

Sample size calculation before the beginning of the study aimed at reaching a study power >80%. To obtain a study power of 85% at least 20 dogs were required, with $\alpha = 0.05$ and mean and SD of the population extrapolated from a pilot study. Statistical analysis was performed using a dedicated statistical software (SPSS[d] v 1.7) and in all cases $P < .05$ was set to indicate statistical significance. Basic descriptive statistical analyses were performed using Microsoft Excel[c] .The Pearson- D'agostino and Shapiro–Wilk tests were used to verify normal distribution of variables. Data with normal distribution were expressed as mean ± standard deviation (SD). For data not normally distributed, median and first and third interquartiles (IQR1-3) were determined.

If the distribution was normal, a paired *t*-test was used to compare the means of 2 continuous variables; the Wilcoxon signed rank test was used with non-normally distributed variables.

For the repeatability study, mean and SD values resulting from postprocessing of repeated examination of dogs with PDA were used for the calculation of within-day and between-day CV (SD of the measurements/average of measurements).

Correlation analysis was performed by means of Pearson's correlation to test for any significant correlation between heart rate and advanced echocardiographic parameters.

Results

Twenty-five dogs with PDA were enrolled in the study, 20 female dogs (80%), and 5 male dogs (20%).

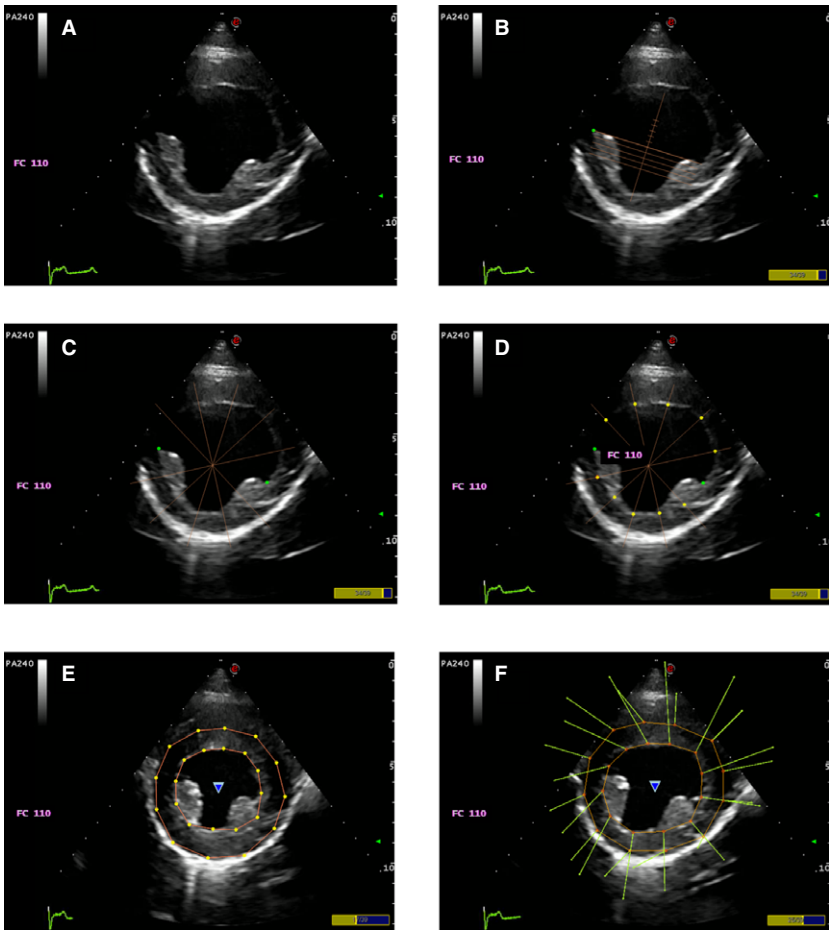

Fig 1. Tracking sequence. The starting points for endocardial tracing (**B**) are manually placed (2 at mid plane), then the software provided tracking guidance by the presence of drawn lines originating from the LV cavity where the endocardial border had to be manually identified and selected (**C** & **D**, a total of 12 points in short axis views). After selecting these points, the software automatically divides the myocardium into segments (**E**), as shown by a continuous line traced, which should follow the endocardial border and is manually adjusted to fit. Velocity vector imaging (VVI) arrows are then displayed above the endocardial border and help evaluating tracking quality during the cardiac cycle : the direction of the arrows indicates the direction of the movement of the left ventricular myocardium and the length of the arrow indicates the velocity of such movement (**F**).

Median age was 12 months (IQR: 6–24 months) and median weight was 13 kg (IQR: 7.5–17.5 kg).

Dog breeds included crossbreeds (5 dogs), Doberman Pinscher and German Shepherd (3 dogs each), Breton, Dachshund and Setter (2 each), and 1 dog each of the following breeds: Bolognese, Bichon Frise, Cocker, Corgi, Labrador Retriever, Newfoundland, Poodle, and West Highland White Terrier.

Mean minimal ductal diameter was 4.6 ± 1.3 mm. All dogs underwent successful percutaneous closure. No complication and no residual flow was observed for any dog. Heart rate decreased 24 hours postoperatively (Table 1).A marked decrease in all standard echocardiographic parameters was observed by 24 hours after percutaneous closure (Table 1).

Standard parameters of diastolic and systolic dimensions ($EDVI_{M/B}$, $ESVI_{M/B}$, AlloD/S) showed a statistically significant decrease 24 hours after percutaneous closure, but none of them was within the normal reference range (Table 1). Furthermore, EF and FS showed statistically significant decreases. Thirteen dogs (52%) had FS values lower than normal, 5 dogs had lower than normal EF_B and 3 dogs also had lower EF_M associated with low EF_B.

The sphericity index showed a statistically significant increase 24 hours after percutaneous closure. As a consequence of PDA closure and of the absence of residual shunting, Qs/Qp ratio normalized (Table 1).

A statistically significant difference in the preoperative and postoperative values of circumferential, radial and transverse S and SR was found (Table 2), with a general decrease in the absolute value, whereas no difference was found for longitudinal S and SR pre- and postoperatively (Table 2).

Epicardial circumferential and longitudinal S and SR had lower absolute values as compared to endocardial ones, a finding that persisted after percutaneous closure (Table 3).

An apex-base gradient was found for longitudinal S and SR, with more negative values for apical segments

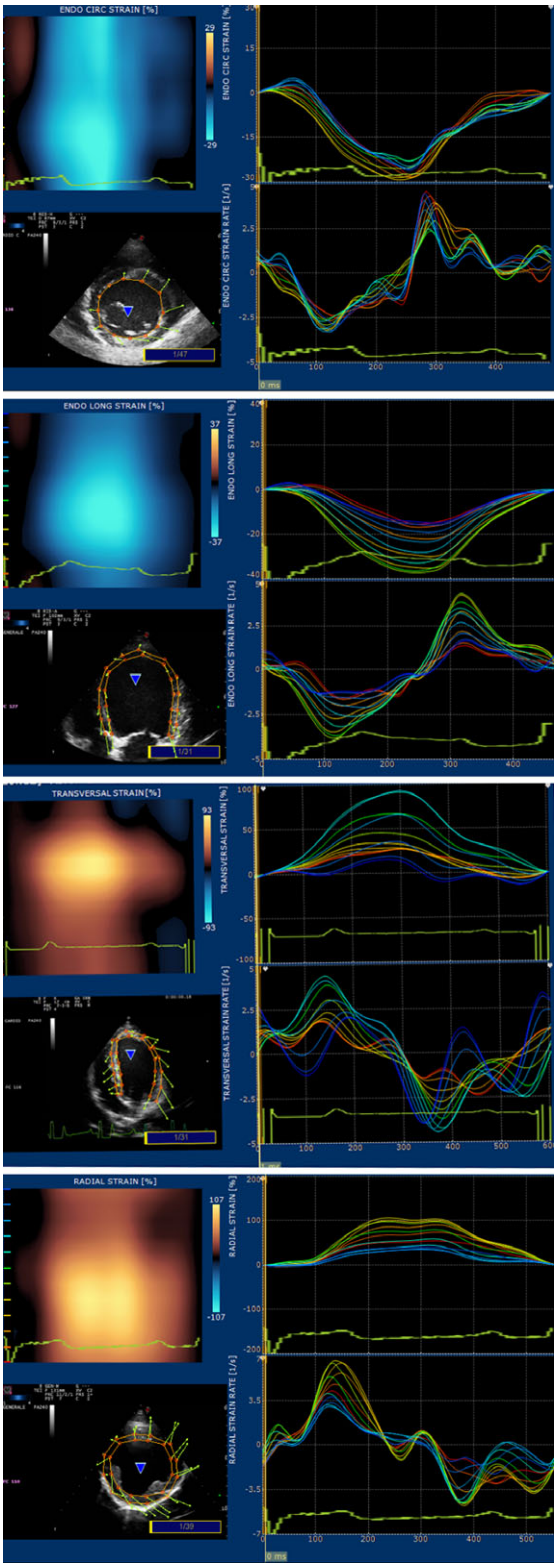

Fig 2. Examples of the graphs originating with STE software. On top, circumferential S and SR, longitudinal S and SR, transversal S and SR, radial S and SR.

and less negative values for basal segments. The apex-base gradient persisted after percutaneous closure (Table 4).

Coefficient of variation in the randomly assessed patients was <0.12 for within-day operator variability and <0.15 for between-day operator variability (Table 5).

No correlation was found between advanced echocardiographic parameters and heart rate.

Discussion

Our study analyzed deformation imaging by means of STE in dogs undergoing percutaneous closure of PDA. Twenty-four hours after ductal closure, statistically significant decreases in all conventional echocardiographic parameters were identified. Circumferential, radial, and transversal S and SR decreased as well, whereas longitudinal S and SR did not change.

Closure of a PDA is associated with marked change in cardiovascular hemodynamics. The presence of a left-to-right PDA is associated with an increase in preload. Afterload plays a relative role in the preclosure hemodynamics but gains importance in the postclosure phase, because preload is decreased and afterload is increased by shunt closure.[6–8,29–31]

These hemodynamic changes were investigated by standard transthoracic echocardiography in previous studies in humans and animals.[11–15,29–34] As a consequence of PDA closure and decreased preload, end-diastolic dimensions ($EDVI_{M\text{-}B}$, AlloD) as well as end-systolic dimensions ($ESVI_{M\text{-}B}$, AlloS) decrease, although they rarely normalize in the short term.[6–8,11–15,29–34] A more pronounced decrease in diastolic dimensions generally is appreciated, whereas systolic dimensions appear to decrease but to a lesser extent as compared to diastolic dimensions after PDA closure.[6,12–14,16–18,34]

This may reflect increased postoperative afterload. The FS and EF values decreased postoperatively as compared to the preoperative evaluation. The results of our study are similar to others in veterinary literature.[11–15] We included M-mode- and B-mode-derived indices of LV end-systolic and end-diastolic dimensions to facilitate comparison with previous data.

Fractional shortening and EF are regarded by most authors as the conventional parameters to evaluate systolic function. They provide information obtained by a change in LV dimensions during the cardiac cycle. Most clinical diseases in cardiology have stable loading conditions, so that EF and FS correctly display cardiac function and are useful tools to investigate pathophysiology. The finding of lower than normal FS and EF in a variable percentage of patients after PDA closure[11–15] led to speculation that these patients may experience systolic dysfunction by PDA closure. However, FS and EF are expected to decrease in this setting because of the combined change in preload and afterload that intrinsically is associated with PDA closure. Any condition associated with a decrease in preload decreases FS, as an increase in afterload also is associated with a decrease in FS.[27] As a consequence, FS and EF also were decreased postoperatively in our study.

The sphericity index (SI) is the ratio between LV internal diameter and LV length; it indicates the ten-

Table 1. Standard echocardiographic parameters in dogs with PDA before and after closure. Results are presented as mean ± SD. Paired *t*-test was performed in all pairs.

Standard echocardiographic parameters	Before closure	After closure	Statistical significance	Reference ranges
Heart Rate (bpm)	121 ± 35	101 ± 23	<0.002	
EDVI M-mode (mL/m^2)	194.88 ± 88.21	132.34 ± 42.77	<0.001	<100
ESVI M-mode(mL/m^2)	78.92 ± 38.81	64.71 ± 28.33	<0.001	<30
EDVI B-mode(mL/m^2)	126.20 ± 61.44	93.53 ± 32.31	<0.001	<70
ESVI B-mode(mL/m^2)	54.74 ± 29.53	50.90 ± 26.22	<0.05	<30
AlloD	2.23 ± 0.41	1.50 ± 0.36	<0.001	1.27–1.85
AlloS	1.43 ± 0.26	1.24 ± 0.25	<0.001	0.71–1.26
SI	1.22 ± 0.15	1.37 ± 0.14	<0.001	>1.65
EF M-mode (%)	59.85 ± 5.56	50.85 ± 12.53	<0.001	>40
EF B-mode (%)	58.09 ± 6.88	47.91 ± 12.89	<0.002	>40
FS M-mode (%)	31.89 ± 3.76	26.20 ± 8.09	<0.001	>25
Qs:Qp	1.88 ± 0.55	0.97 ± 0.13	<0.001	0.8–1.2
PDA minimal ductal diameter (mm)	4.6 ± 1.34			

Table 2. Advanced echocardiographic parameters in dogs with PDA before and after closure. Results are presented as mean ± SD. Paired *t*-test was performed in all pairs. NS: *P* value >.05.

Advanced echocardiographic parameters	Before closure	After closure	Statistical significance
Circumferential S (%)	−26.87 ± 5.29	−21.16 ± 5.48	<0.001
Circumferential SR (/s)	−3.11 ± 0.79	−2.46 ± 0.99	<0.001
Radial S (%)	52.17 ± 18.71	37.52 ± 10.56	<0.001
Radial SR (/s)	4.29 ± 1.32	3.08 ± 0.93	<0.001
Longitudinal S (%)	−19.15 ± 5.99	−18.57 ± 4.25	NS
Longitudinal SR (/s)	−2.17 ± 0.75	−2.15 ± 0.55	NS
Transversal S (%)	51.13 ± 18.03	33.92 ± 13.52	<0.001
Transversal SR (/s)	4.51 ± 1.03	3.62 ± 0.91	<0.001

Table 3. Endocardial and Epicardial longitudinal and circumferential S and SR. Results are presented as mean ± SD. Paired *t*-test was performed in all pairs.

	Before closure	After closure	*P* value
Endocardial circumferential S	−27.7 ± 4.0%	−24.1 ± 8.4%	<.01
Endocardial circumferential SR	−3.26 ± 0.83/s	−2.82 ± 1.31/s	<.04
Epicardial circumferential S	−12.17 ± 2.39%	−8.8 ± 3.21%	<.001
Epicardial circumferential SR	−1.20 ± 0.35/s	−0.85 ± 0.29/s	<.001
Endocardial longitudinal S	−19.15 ± 5.99%	−18.57 ± 4.25%	<.01
Endocardial longitudinal SR	−2.17 ± 0.67/s	−2.15 ± 0.55/s	<.01
Epicardial longitudinal S	−18.2 ± 4.6%	−15.7 ± 5.7%	<.02
Epicardial longitudinal SR	−2.31 ± 0.67/s	−1.83 ± 0.65/s	<.01

dency of the LV to acquire a spherical shape when the ratio is <1.65.[27] Dogs with PDA had lower than normal SI before PDA closure, and although SI was shown to increase significantly after ductal closure, even postoperatively it was below the reference range, indicating that the LV had a more spherical shape as compared to normal hearts.

Speckle tracking echocardiography allows quantification of myocardial contractility by the analysis of myocardial deformation during the cardiac cycle. In a previous study[c] all S and SR parameters were increased in dogs with PDA as a consequence of LV overload in the preoperative setting. At least initially, the increase in preload will enhance cardiac contractility, balancing increased blood flow in the LV as well as blood escape through the shunt (Frank–Starling Law).

After PDA closure, a statistically significant decreases in circumferential, radial and transverse S and SR were observed. The sudden decrease in these deformation parameters 24 h after PDA closure may reflect a decrease in preload related to PDA closure. Laplace's law states that tension on the myocardial wall is directly dependent on LV pressures and the radius of the LV divided by LV free wall thickness.[35] If preload decreases after PDA closure, the tension on the myocardial wall decreases as well as the radius of the LV, both of which will lead to a decrease in the strength of contraction of the circumferential and radial fibers following the Frank–Starling mechanism.

The values obtained postoperatively were similar to those obtained in healthy control dogs in previous studies[c], thus, it could be argued that PDA closure immediately restores the contractility pattern of the circumferential fibers of the LV. Radial, transverse, and circumferential S and SR could be considered as markers of short axis function, because these parameters

Table 4. Segmental Longitudinal S and SR values pre- and postoperatively. Results are presented as mean ± SD. A base to apex gradient can be appreciated.

	Basal septal	Mid septal	Apical septal	Apical lateral	Mid lateral	Basal lateral	Overall
Longitudinal S pre	−15.38 ± 5.68%	−18.00 ± 5.72%	−20.98 ± 6.26%	−21.22 ± 6.44%	−20.14 ± 5.99%	−19.21 ± 5.81%	−19.15 ± 5.99%
Longitudinal S post	−14.87 ± 3.61%	−17.97 ± 4.26%	−21.13 ± 4.16%	−22.18 ± 5.01%	−18.38 ± 4.61%	−16.09 ± 3.87%	−18.57 ± 4.25%
Longitudinal SR pre	−1.96 ± 0.52/s	−2.14 ± 0.69/s	−2.38 ± 0.74/s	−2.29 ± 0.78/s	−2.14 ± 0.68/s	−2.12 ± 0.59/s	−2.17 ± 0.67/s
Longitudinal SR post	−1.71 ± 0.47/s	−2.19 ± 0.53/s	−2.38 ± 0.60/s	−2.58 ± 0.65/s	−2.21 ± 0.58/s	−1.83 ± 0.51/s	−2.15 ± 0.55/s

evaluate the motion of the circumferential fibers belonging to the basal loop, as described previously.[36]

In our case series, all parameters related to short axis function normalized 24 h after percutaneous closure. No data are available for comparison regarding STE-derived parameters in infants with PDA and short axis deformation imaging.

On the other hand, longitudinal S and SR did not show a statistically significant decrease in the postoperative setting. Longitudinal fibers are predominant in the endocardium and are oriented in a base-apex conformation, contributing mainly to the apical loop.[36]

Longitudinal fibers are particularly susceptible to ischemia because of the fact that the myocardium is perfused from the epicardium to the endocardium.[16] Decreases in longitudinal S and SR are associated with an early decrease in systolic function in various disease conditions in humans,[16,20] even in human infants with PDA.[29,31,34] In human patients, global longitudinal S decreased to lower than normal values 24 h postoperatively,[29] and subsequently increased in the long term (ie, 6 months after PDA closure). Another study in preterm infants undergoing surgical ligation identified a similar decrease in global long S and SR as early as 1 hour after PDA closure, but the same parameters showed an increase 18 hours postoperatively.[34] Preterm infants treated with indomethacin showed a smaller decrease in global long S and SR 10 minutes after indomethacin infusion and an increase in long S and SR 60 minutes after the infusion. Cyclo-oxygenase inhibitors, however, induce an increase in prostaglandin concentration, which in turn will cause ductal constriction and an increase in vascular resistance as a consequence of generalized vasoconstriction.[37] In our case series, longitudinal S and SR were slightly lower as compared to preclosure, but were higher as compared to a normal population of dogs in which STE was assessed by the same software[38e] Whether this difference between infants and dogs is associated with different cardiac mechanics (preterm infants are considered to have decreased myocardial reserve[39] and are thus more susceptible to changes in loading condition, requiring vasopressor or inotrope support[31]) or caused by a different timing for these changes to occur, is difficult to determine. Based on our data, systolic dysfunction, considered as a decrease in myocardial contractility, has not been observed 24 h postoperatively in our population of dogs with PDA.

Left ventricular reverse remodeling refers to the possibility of restoring cardiac morphology and function after treatment for a particular disease condition that has modified LV anatomy.[40] Left ventricular remodeling eventually can cause changes in LV shape and function, although it is a complex process, starting from cellular and extracellular pathways.

Normalization of the echocardiographic parameters of LV dimension and function has been reported in preterm infants[30] and in veterinary patients.[14] The finding that all of the cardiovascular changes associated with a PDA seemed reversible once the PDA was closed[30] suggests that LV remodeling could be a reversible process, but it is unclear when this occurs.

Table 5. Coefficient of variation for advanced echocardiographic parameters.

CV	Circ S	Circ SR	Rad S	Rad SR	Long S	Long SR	Transv S	Transv SR	Global CV
Between day	0.11	0.13	0.18	0.15	0.12	0.14	0.18	0.16	0.146
Within day	0.08	0.10	0.15	0.14	0.09	0.10	0.16	0.14	0.12

Our case series showed a significant postoperative decrease in all standard echocardiographic parameters, but none of the parameters considered were within reference ranges 24 h after PDA closure, indicating that this is not an immediate process and requires time. Different echocardiographic parameters can be taken into account to assess whether long-term remodeling occurs, including standard and advanced echocardiographic parameters. With particular regard to STE, global longitudinal strain was found to be a marker of effective reverse remodeling (defined as a decrease in <15% of LV inner diameters) in patients undergoing cardiac resynchronization treatment and transcatheter aortic valve implantation.[41] Long-term studies therefore are required to investigate reverse remodeling in dogs with PDA.

Our study identified basal to apical gradients in longitudinal S and SR and a difference between epicardial and endocardial S and SR in dogs with PDA, as described in healthy humans[42] and dogs.[38] Endocardial circumferential and longitudinal S and SR are greater as compared to their epicardial counterparts. Based on these findings, PDA did not change the normal segment contraction patterns.

Repeatability was acceptable for global S and SR values, with the highest CV for radial and transverse S and SR. Circumferential and longitudinal S and SR had better reproducibility in our case series. Global longitudinal S and SR are considered strong robust parameters and the ones with better reproducibility in human cardiology[43] as well.

Our study had some limitations. The prospective nature of the study enabled homogeneous data to be acquired, but some other data or techniques, that could have proven interesting to compare (eg, tissue Doppler imaging [TDI] values, velocity of circumferential fiber shortening, magnetic resonance imaging), were not acquired, but these measurements were beyond the scope of our study. The decision to evaluate patients 24 h after percutaneous closure was based on a routine clinical re-examination performed at the referral center where the study was carried out, however, more frequent re-examinations may be required in order to identify whether conventional and advanced echocardiographic parameters show earlier changes and, if so, characterize the trend in the echocardiographic parameters over time. Furthermore, patient number was acceptable according to the study design but not very high, so that additional studies with a larger number of patients may be needed. Long-term follow-up was not available, which represents another limitation of our study.

In conclusion, PDA closure with percutaneous technique causes decreases in conventional echocardiographic parameters of LV dimension and function, but a definitive or transient systolic dysfunction was not identified by means of STE in our cohort of patients. After PDA closure, the circumferential fibers in the LV restore a normal pattern of contraction, as shown by the normalization of circumferential, transversal, and radial S and SR, whereas longitudinal fibers, although not damaged by the persistent PDA-induced LV overload, do not decrease their contractility pattern and persistently have higher than normal values.

Footnotes

[a] ACDO©, Amplatzer Canine Duct Occluder, Infinity Medical, Menlo Park, California, USA

[b] XStrain© software, Firenze, Italy

[c] Microsoft Excel©, Microsoft Corporation Redmond, Washington, USA

[d] SPSS statistic©; IBM Corporation Armonk, New York, USA

[e] Spalla I, Locatelli C, Bussadori C et al. Speckle tracking echocardiography in dogs with patent ductus arteriosus. 23rd ECVIM congress, Liverpool (UK).

[f] Esaote © MyLab 50 and Class C, Firenze, Italy

Acknowledgments

Conflict of Interest Declaration: Dr. Bussadori receives royalties from ESAOTEf 37 related to a European patent (nr 071129712) he developed for Xstrain software.

Off-label Antimicrobial Declaration: Authors declare no off-label use of antimicrobials.

References

1. Clyman RI. Mechanisms regulating the ductus arteriosus. Biol Neonate 2006;89:330–335.

2. Buchanan JW. Causes and prevalence of cardiovascular disease. In: Kirk RW, Bonagura JD, eds. Kirk's Current Veterinary Therapy XI. Philadelphia, PA: WB Saunders, 1992:647–655.

3. Buchanan JW. Prevalence of cardiovascular disorders. In: Fox R, Sisson D, Moïse NS, eds. Textbook of Canine and Feline Cardiology, 2nd ed. Philadelphia: Saunders; 1999:457–463.

4. Tidholm A. Retrospective study of congenital heart defects in 151 dogs. J Small Anim Pract 1997;38:94–98.

5. Oliveira P, Domenech O, Bussadori C, et al. Retrospective review of congenital heart disease in 976 dogs. J Vet Int Med 2011;25:477–483.

6. Kittleson MD. Patent Ductus Arteriosus. In: Kittleson MD, Kienle RD, eds. Small Animal Cardiovascular Medicine. St Louis Mosby; 1998:494–522.

7. Buchanan JW. Patent Ductus Arteriosus. In: Fox R, Sisson D, Moïse NS, eds. Textbook of Canine and Feline Cardiology, 2nd ed. Philadelphia: Saunders; 1999:505–512.

8. Kittleson MD. Pathophysiology of heart failure. Heart failure secondary to patent ductus arteriosus. In: Kittleson MD, Kienle RD, eds. Small Animal Cardiovascular Medicine. St Louis: Mosby; 1998:329–334.

9. Nguyenba TB, Tobias AH. The Amplatz Canine Duct Occluder: a novel device for patent ductus arterious closure. J Vet Cardiol 2007;9:109–117.

10. Singh M, Kittleson M, Griffiths L, et al. Occlusion devices and approaches in canine patent ductus arteriosus: comparison of outcomes. J Vet Int Med 2012;26:85–92.

11. Van Israel N, French A, Corcoran B, et al. Review of left to right shunting patent ductus arteriosus and short term outcome in 98 dogs. J Small An Pract 2002;43:395–400.

12. Van Israel N, Dukes McEwan J, French A. Long term follow up of dogs with patent ductus arteriosus. J Small An Pract 2003;44:480–490.

13. Campbell F, Thomas W, Kittleson M, et al. Immediate and late outcomes of transarterial coil occlusion of patent ductus arteriosus in dogs. J Vet Int Med 2006;20:83–96.

14. Stauthammer C, Tobias A, Krüger M. Structural and functional cardiovascular changes and their consequences following interventional patent ductus arteriosus occlusion in dogs: 24 cases (200-2006). J Am Vet Med Ass 2013;242:1722–1726.

15. Saunders A, Gordon S, Miller M, et al. Long-term outcome in dogs with patent ductus arteriosus: 520 cases (1994-2009). J Vet Int Med 2014;28:401–410.

16. Steeds R. Echocardiography: frontier imaging in cardiology. British J Rad 2011;84:S237–S244.

17. Blessberger H, Binder T. Two-dimensional speckle tracking echocardiography: basic principles. Heart 2010;96:716–722.

18. Bijnens BH, Cikes M, Sutherland G, et al. Velocity and deformation imaging in the assessmentof myocardial dysfunction. Eur J Echocard 2009;10:216–226.

19. Dandel M, Lehmkuhl H, Hetzer R, et al. Strain and strain rate imaging by echocardiography: basic concepts and clinical applicability. Curr Cardiology Rev 2009;5:133–148.

20. Biswas M, Sudhakar S, Houle H, et al. Two- and Three-Dimensional Speckle-Tracking echocardiography: clinical application and future directions. Echocardiography 2013;30:88–105.

21. Carabello B. Evolution of the Study of Left Ventricular Function: Everything Old Is New Again. Circulation 2002;105: 2701–2703.

22. Chetboul V. Advanced echocardiographic techniques in echocardiography in small animals. Vet Clin North Am Small An Pract 2010;40:529–543.

23. Lang RM, Badano LP, Voigt JU, et al. Recommendations for cardiac chamber quantification by echocardiography in adults: an update from the American society of echocardiography and the European Association of Cardiovascular Imaging. J Am Soc Echocardiogr 2015;28:1–39.

24. Thomas WP, Gaber CE, Moses BL, et al. Recommendations for standards in transthoracic two-dimensional echocardiography in the dog and cat. Echocardiography Committee of the Specialty of Cardiology, American College of Veterinary Internal Medicine. J Vet Int Med 1993;7:247–252.

25. Cornell CC, Kittleson MK, Wey A. Allometric scaling of M-mode cardiac measurements in healthy dogs. J Vet Int Med 2004;18:311–321.

26. Sanders SP, Yeager S, Williams RG. Measurement of systemic and pulmonary blood flow and QS/QP ratio using doppler and two-dimensional echocardiography. Am J Cardiol 1983;51: 952–969.

27. Boon J. Evaluation of size, function and hemodynamics. In: Boon J, ed. Veterinary Echocardiography 2011, 2nd ed. Chichester, UK: Wiley Blackwell; 2011:153–266.

28. Voigt JU, Pedrizzetti G JD, Badano LP. Definitions for a common standard for 2D speckle tracking echocardiography: consensus document of the EACVI/ASE/Industry Task Force to standardize deformation imaging. J Am Soc Echocardiogr 2015;28: 183–193.

29. Amoogzar H, Shakiba AM, Mehdizadegan N. Evaluation of left ventricular function by tissue Doppler and speckle-derived Stran rate echocardiography after percutaneous ductus closure. Pediatr Cardiol 2015;36:219–225.

30. Eerola A, Jokinen E, Pikhala J, et al. The Influence of Percutaneous Closure of Patent Ductus Arteriosus on Left Ventricular Size and Function. J Am College of Cardiol 2006;47:1060–1066.

31. Noori S. Pros and cons of patent ductus arteriosus ligation: hemodynamic changes and other morbidities after patent ductus arteriosus ligation. Semin Perinatol 2012;36:139–145.

32. Gupta S, Krishnamooorthy K, Anees T, et al. Percutaneous closure of patent ductus arteriosus in children: immediate and short term changes in left ventricular systolic and diastolic function. Ann Pediatr Cardiol 2011;4:139–144.

33. Jeong Y-H, Yun T-J, Song J-k, et al. Left ventricular remodelling and change of systolic function after closure of patent ductus arteriosus in adults: device and surgical closure.

34. El khuffash AF, Jain A, Mertens L, et al. Acute changes in myocardial systolic function in preterm infants undergoing patent ductus arteriosus ligation: a tissue Doppler and myocardial deformation study. J Am Soc Echocardiogr 2012;25:1058–1067.

35. Hamlin R. Normal cardiovascular physiology. In: Fox R, Sisson D, Moïse NS, eds. Textbook of Canine and Feline Cardiology, 2nd ed. Philadelphia: Saunders; 1999:25–37.

36. Torrent-Guasp F, Kocica M, Wen H, et al. Towards new understanding of the heart and function. Eur J of Cardio Thor Surgery 2005;27:191–201.

37. Sehgal A, Doctor T, Menahem S. Ciclooxygenase inhibitors in preterm infants with Patent Ductus Arteriosus: effects on cardiac and vascular indices. Pediatr Cardiol 2014;34:1429–1436.

38. Carnabuci C, Hanås S, Höglund K, et al. Assessment of cardiac functions using global and regional left ventricular endomyocardial and epimyocardial peak systolic strain and strain rate in healthy Labrador retriever dogs. Res Vet Sci 2013;9:241–248.

39. Barlow A, Ward C, Sandor G, et al. Myocardial contractility in premature neonates with and without patent ductus arteriosus. Pediatr Cardiol 2004;25:102–107.

40. Koitabashi N, Kass D. Reverse remodeling in heart failure: mechanisms and therapeutic strategies. Nat Rev Cardiol 2012;9:147–157.

41. Park J, Negishi K, Marwick T, et al. Echocardiographic predictors of reverse remodeling after cardiac resynchronization therapy and subsequent events. Circ Cardiovasc Imaging 2013;6: 864–872.

42. Bussadori C, Moreo A, Carminati M, et al. A new 2D-based method for myocardial velocity strain and strain rate quantification in a normal adult and pediatric population: assessment of reference values. Cardiovasc US 2009;7:8.

43. Risum N, Ali S, Kisslo J, et al. Variability of global left ventricular deformation analysis using vendor dependent and independent two-dimensional speckle-tracking software in adults. J Am Society of Echocardiogr 2012;25:1195–1203.